



### **Science Arts & Métiers (SAM)**

is an open access repository that collects the work of Arts et Métiers Institute of Technology researchers and makes it freely available over the web where possible.

This is an author-deposited version published in: <https://sam.ensam.eu>  
Handle ID: <http://hdl.handle.net/10985/17001>

#### **To cite this version :**

Cyril NICOLAS, Cyrille BAUDOUIN, Stéphane LELEU, Mihaela TEODORESCU - Dimensional control strategy and products distortions identification - International Journal of Material Forming - Vol. 1, n°Supplement 1, p.1039-1042 - 2008

Any correspondence concerning this service should be sent to the repository

Administrator : [scienceouverte@ensam.eu](mailto:scienceouverte@ensam.eu)



# Dimensional control strategy and products distortions identification

C. Nicolas<sup>1</sup>, C. Baudouin<sup>1</sup>, S. Leleu<sup>2</sup>, M. Teodorescu<sup>3</sup>, R. Bigot<sup>1</sup>

<sup>1</sup> *Laboratoire de Génie Industriel et Production Mécanique (LGIPM – IFAB)*  
*Ecole Nationale Supérieure d'Arts et Métiers - C.E.R de Metz - 4, rue Augustin Fresnel - 57078 Metz Cedex3*  
<http://www.metz.ensam.fr/> {cyril.nicolas, cyrille.baudouin, regis.bigot}@metz.ensam.fr;

<sup>2</sup> *Laboratoire de Métrologie et Mathématiques Appliquées (L2MA)*  
*Ecole Nationale Supérieure d'Arts et Métiers - C.E.R de Lille - 8, boulevard Louis XIV - 59046 Lille Cedex*  
<http://www.lille.ensam.fr/> stephane.leleu@lille.ensam.fr;

<sup>3</sup> *ASCOMETAL CREAS - BP 70045 - 57301 - Hagondange Cedex*  
*m.teodorescu@ascometal.lucchini.com*

**ABSTRACT:** Heat treatments could create local or global distortions on workpieces. Finishing operations, often costly, are then necessary to respect the required functional tolerances. In the long term, our objective is to optimize first, steel grade and heat treatment, then to adjust the numerical simulation models. In that way, the heat treatment distortions on C-ring test parts obtained for an ASCOMETAL steel grade, vertically gas quenched are qualified and quantified by a dimensional analysis. In this article, we focus on part measurement and data processing strategies. Then we present an approach to correlate the experimental results with simulations ones.

**Key words:** Distortions, Heat treatments, Metrology, Dimensional analysis, Numerical simulation

## 1 INTRODUCTION

Our work is focussed on heat treatment process which is used to improve product mechanical properties (e.g. hardness, strength). These heat treatments may cause undesirable dimensional changes. Finishing operations are then needed; hence distortions control could help minimizing the rise in cost. Distortions prediction is however complex because depending on many parameters (thermo mechanical, metallurgical), which are, mostly, experimentally estimated.

In this paper, we propose a distortions control strategy using metrological and simulation analyses. The first part reviews some literature methods to identify heat treatments distortions. Then, we introduce our method with data processing coming from measurements and simulations. The third part presents first results for an ASCOMETAL steel grade.

## 2 DISTORTIONS IDENTIFICATION METHOD

### 2.1 Existing methods

Within the framework of heat treatments, two main and complementary approaches are found in the literature.

#### 2.1.a Deductive approach

It consists in checking distortions predictive models via experimentations and simulations. A knowledge based system could be used [1]. Distortions are quantified on parts families for which are associated potential distortions (e.g. banana effect) and distortions generating factors such as part geometry, metallurgical properties, place in the furnace, cooling fluid characteristics. One can also find other foretelling models using these distortions factors but individually considered; as the part geometry [2] for which a correlation method was developed.

However, finite element models (f.e.m.) are the most used because they help us to understand distortions origin through metallurgical and thermo mechanical phenomena analyses. Like all numerical models, the results accuracy greatly depends on the quality of the input data. In addition to simulation based approach, it is thus necessary to perform experiments to corroborate preliminary results. In that way, distortions simulation accuracy was improved on carburizing-quenching gear by experimentally determining materials thermal

properties [3].

### 2.1.b Inductive approach

It consists in proposing models to identify distortions coming from experiment, mainly from metrology. So, we need to define the number and distribution of points so that significant surfaces for the optimization criterion would be measured with the smallest possible loss of information [4]. The number of points is subject to part size, tolerance specifications and measurement uncertainty. The theoretical smallest sampling size can be used for ideal geometric shape identification. But, if the form deviation is unknown (that is our case), we have to increase the sampling size so that estimated value of the measurement converges to the “true” value of form error [5]. As for points distribution, for not creating local weighting disturbing the optimization method, it is important to dispose them uniformly. Next, we need an optimization criterion to resolve this “data-overabundant” system. In our case of warped surfaces identification, a point-per-point comparison between measured and theoretical geometry is needed [6]. We chose the least squares criterion because it gives a very stable result and is less sensitive to asperities effects [7].

## 2.2 Developed method

### 2.2.a Introducing C-ring test part

The C-ring type sample is currently used because its geometry allows us to amplify distortion which is suitable for the metrological analysis [8] [9]. We use a 100 mm long C-ring with a 16 mm wide opening. Outer and inner cylinders (respectively Ø70 and Ø45 mm) are 11 mm off-centered. These dimensions authorize thermocouples without disturbing thermal flow; they minimize side effects and allow obtaining required cooling velocity [10].

First, a metrological analysis occurs at three manufacturing states: after machining, after stress relieving and after high pressure gas quench. Then, we present a method to correlate C-ring measured mesh with f.e.m. one in order to compare simulate distortions field with measurement’s one.

### 2.2.b Experiment approach

#### Measurement strategy

In order to characterise the distortions significant types, we define a fine mesh for the C-ring. We keep in mind that many measurement points may increase the appearance of abnormal points but we could detect them via a graphic interface (see section 3).

Points are evenly distributed on all surfaces (figure 1), but not on the putting plane (bottom one).

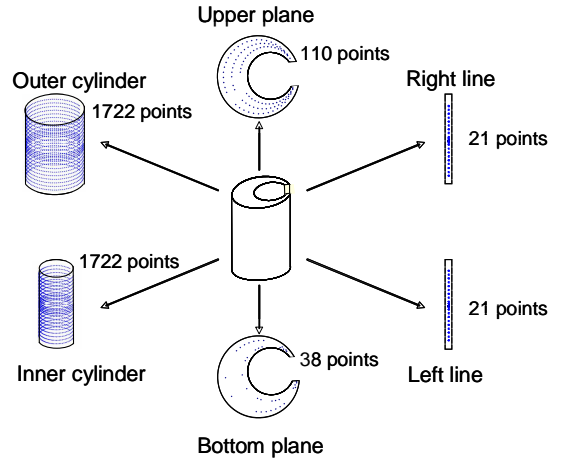


Fig. 1. Fine mesh for points probing

#### Data processing strategy

Our mathematic approach is to optimize, for each point  $i$ , the measure error  $\varepsilon_i$  between theoretical point  $T_i$  and measured point  $M_i$ , orthogonally projected onto theoretical normal  $N_i$  (equation (1)).

$$\text{In reference frame } (\vec{O}, \vec{i}, \vec{j}) \quad \vec{\varepsilon} = \begin{pmatrix} \varepsilon_1 \\ \vdots \\ \varepsilon_i \\ \vdots \\ \varepsilon_n \end{pmatrix} \quad \text{with } \begin{cases} \varepsilon_i = (\vec{OT}_i - \vec{OM}_i) \cdot \vec{N}_i \\ \|\vec{N}_i\| = 1 \end{cases} \quad (1)$$

We also define the matrix  $M_{ph}$  of optimization phenomena (equation (2)). Its scalars correspond to the phenomena elementary amplitude effect ( $e_{ph_{nj}}$ ) on the theoretical points written in column. The description unit of phenomena would be close to their estimated value, so the millimetre.

$$M_{ph} = \begin{matrix} & \begin{matrix} T_x & T_y & \dots & Ph_n \end{matrix} \\ \begin{matrix} OT_1 \\ \vdots \\ OT_j \\ \vdots \\ OT_n \end{matrix} & \begin{matrix} e_{Tx_1} & e_{Ty_1} & \dots & e_{Ph_{n1}} \\ \vdots & \vdots & \vdots & \vdots \\ e_{Tx_j} & e_{Ty_j} & \dots & e_{Ph_{nj}} \\ \vdots & \vdots & \vdots & \vdots \\ e_{Tx_n} & e_{Ty_n} & \dots & e_{Ph_{nn}} \end{matrix} \end{matrix} \quad \text{with } \begin{cases} \|\vec{T_x}\| = \|\vec{T_y}\| = 1mm \\ e_{Tx_j} = \vec{T_x} \cdot \vec{N_j} = \vec{N_j} \cdot \vec{x} \\ e_{Ty_j} = \vec{T_y} \cdot \vec{N_j} = \vec{N_j} \cdot \vec{y} \end{cases} \quad (2)$$

To dissociate phenomena, those must be mathematically independent and linearly superimposable. In metrology, the size order of the defects is often small compared with nominal dimensions of the measured part and so, we will use the small displacements assumption.

Finally, equation (3) gives the residual  $r$  to minimize using the least square criteria thanks to any solver.

$$r = \left\| \vec{\varepsilon} - a.\overrightarrow{Ph_1} - b.\overrightarrow{Ph_2} - c.\overrightarrow{Ph_i} - \dots - n.\overrightarrow{Ph_n} \right\| \quad (3)$$

with elementary quantities (a, b, c, ..., n) of significant displacements and distortions phenomena ( $\overrightarrow{Ph_1}, \dots, \overrightarrow{Ph_n}$ )

### Experimental device

Our coordinate measuring machine (CMM) has an indication error for length measurement defined by  $E = (3.5 + L/350) \mu m$ , L in mm.

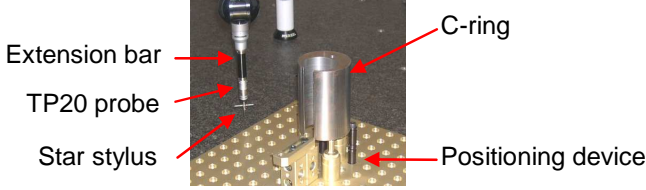


Fig. 2. Experimental control device

We use a dynamic probe (TP20) with a star stylus and an extension bar (figure 2). Combined with probe head rotations, we can access all surfaces. But, even with rotations, we do not obtain a uniform distribution of points for the inner cylinder. We thus checked the accuracy of our device compared with a single TP20 probe (without extension bar and star stylus) in measuring a 44.99mm standard ring (table1). To succeed, we optimize the 108 points of CMM with Tx-Ty and dilatation vectors.

Table1. CMM measurements of a standard ring diameter

Values in mm	Single TP20	Our TP20 device
Diameter	44.989	44.989
Range	0.006	0.005

### 2.2.c Processing of finite element simulation

We use Forge 2005 software to make 3D-quench simulations for which the input data are partly experimentally determined (the phase transformation kinetics, the heat transfer coefficient) and partly from the literature (the mechanical data) [12].

### Data processing strategy

For a direct comparison between experimental and simulation results, we use the method previously presented. For instance, this method is applied for only the cylinders. By using “2D-cutting planes”, we export sections’ boundary geometry at the same heights as for CMM measured C-ring. However, we must keep in mind that CMM measurement points are obtained by probing the surface following the theoretical normals. But during simulation, nodes move on all directions. So, we have to find the intersection point  $S_{12}$  between theoretical normals  $T_1$  and finite element frontier ( $S_1 S_2$ ).

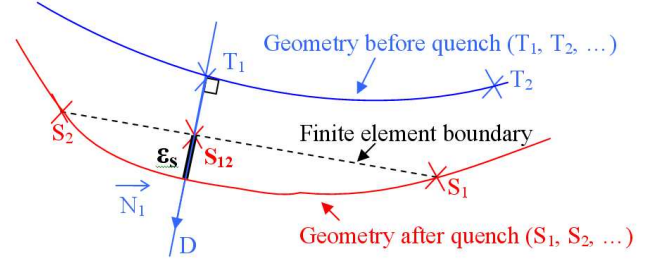
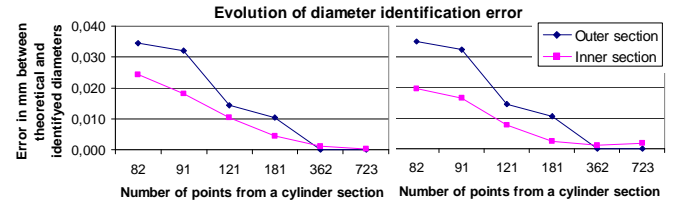


Fig. 3. Intersection point  $S_{12}$  between ( $S_1 S_2$ ) and D lines

### Uncertainty due to the method

The method generates a quantifiable error  $\varepsilon_s$  due to the linear approximation between two consecutive nodes of the finite element frontier (figure 3). To minimise this error, we look for the 2 simulation points ( $S_1$  and  $S_2$ ) whose angular coordinates are as close as possible to theoretical point ( $T_1$ ) ones. In figure 4, we show that higher is the sampling size; higher is the accuracy. This last also increase when the diameter size is smaller for the same sampling size.



Case 1: Simulation nodes are theoretical points of outer and inner diameters

Case 2: Simulation nodes are theoretical points of dilated diameters (0.5mm)

Fig. 4. Uncertainty due to data processing of simulation points

### Initial geometry for quench simulation

We must take into account C-ring dilation due to heating (at 930 °C). We consider for the studied steel grade a linear dilatation value of  $22.3 \mu m/m/^\circ C$  in austenitic phase. Then, we create the same mesh as for experimental analysis, consisting of 98 sections with 400 nodes for each cylinder’s perimeter. This fine mesh aims to minimize the uncertainty of our method.

## 3 FIRST RESULTS

A software based on the described method was developed. Thus, numerical and 3D-identification of distortions phenomena can be calculated. For a better visual understanding, a scale factor is applied on the errors onto the theoretical normals (figure 5). Theses measure errors include displacements phenomena, like translations, rotations and off-centring of the inner diameter (due to machining). By deleting them, we did what is often called *best*



fit, to better visualize distortion and to write their 3D-mathematical expression (figure 6).

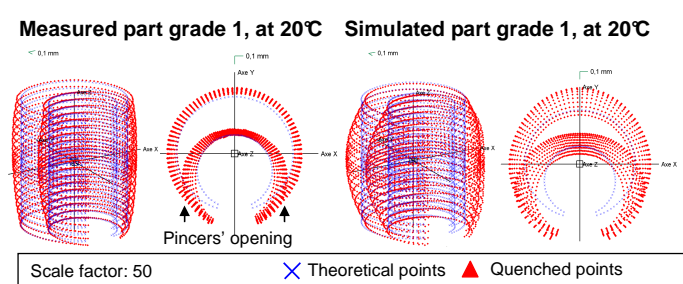


Fig. 5. Graphic comparison of best-fitted quenched geometries

All phenomena have physical origins, as the pincers' opening which comes from a gradient of thermal stresses induced by the thickness and temperature gradients and the steel phase transformations.

Phenomena	Mathematical expressions	Vectors effects on errors onto theoretical normals
Ovalization (also dilation)	<p><b>For each section :</b></p> $e_{oval_{xj}} = N_j \cdot N_{j,x} \cdot x = N x_j^2$ $e_{oval_{y_j}} = N y_j^2$	<p>Theoretical points Scale factor = 5</p>
Pincers' opening (or closing)	<p><b>For each section :</b></p> $e_{open_j} = 1 - \cos \frac{\alpha_j}{2}$ $\alpha_j = -Atan2(OT_{j,y}; OT_{j,x})$	<p>Theoretical points Scale factor = 5</p>
Barrel (or bobbin)	<p><b>For each generatrix :</b></p> $e_{barrel_j} = 1 - z_j^2$ $z_j = -1 + 0.1 \times k, k \in [0,20]$	<p>Theoretical points Scale factor = 5</p>
Banana	$\begin{cases} \text{If } y_{ci} \geq 0; e_{banana_j} = N y_j^2 \times e_{barrel_j} \\ \text{If } y_{ci} < 0; e_{banana_j} = -N y_j^2 \times e_{barrel_j} \end{cases}$	<p>Theoretical points Scale factor = 5</p>

Fig. 6. Linear and independent 3D-distortion phenomena

A comparison between experimental and simulation results (figure 7) show that distortions values of the outer cylinder are greater than inner ones (except for barrel effect). Pincers' opening is the most important phenomenon in experiment just as barrel and banana effects in simulation.

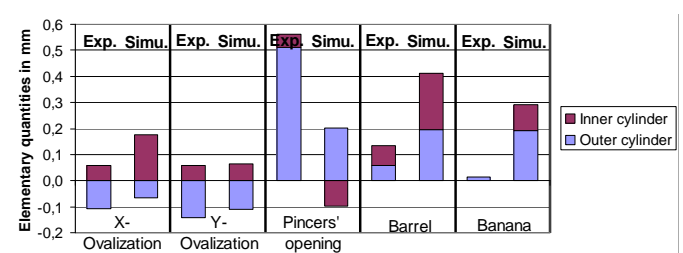


Fig. 7. Results for 3D-distortions identification from experiment and simulation

The chosen vectors for phenomena explain the main distortions as the final residual is small (figure 8).

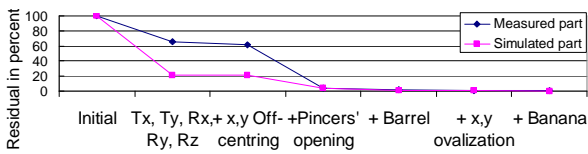


Fig. 8. Residual evolution in function of cumulated phenomena

## 4 CONCLUSIONS

We developed a method for identifying distortions based on the optimisation of the measure errors by the mean of distortions significant phenomena. In this first approach, tendencies of these phenomena are quite the same in experiment and simulation but we have to refine input data of the models for a better quantitative evaluation. Further work will focus on many experiments and on simulations including mechanical experimental data.

## REFERENCES

1. P. Lamesle, E. Vareilles and M. Aldanondo, Towards a KBS for a Qualitative Distortion Prediction for Heat Treatments, In: *Proc. 1<sup>st</sup> Int. Conference on Distortion Engineering*, Bremen (2005) 39-47.
2. C. Andersch, M. Ehlers, F. Hoffmann and H.-W. Zoch, 'Systematic Analysis of the Relation between Part Geometry and Distortion due to Heat Treatment', *Mat.-wiss. u. Werkstofftech.*, 37, (2006) 23-28.
3. R. Mukai and D.-Y. Ju, 'Simulation of Carburizing-Quenching of a Gear. Effect of Carbon Content on Residual Stresses and Distortion', *Journal de Physique IV*, 120, (2004) 489-497.
4. A. Weckenmann and M. Knauer, The Influence of Measurement Strategy on the Uncertainty of CMM-Measurements, *Annals of the CIRP*, 47, (1998) 451-454.
5. G. Lee, J. Mou and Y. Shen, 'Sampling Strategy Design for Dimensional Measurement of Geometric Features Using Coordinate Measuring Machine', *Int. Journal of Machine Tools and Manufacture*, 37, (1997) 917-934.
6. C. Baudouin, R. Bigot, S. Leleu and P. Martin, 'Gear Geometric Control Software: Approach by Entities', *Int. Journal of Advanced Manufacturing Technology*, 2007.
7. H.T. Yau and C.H. Menq, 'A Unified Least-Squares Approach to the Evaluation of Geometric Errors using Discrete Measurement Data', *Int. Journal of Machine Tools and Manufacture*, 36, (1996) 1269-1290.
8. R.A. Hardin and C. Beckermann, Simulation of Heat Treatment Distortion, In: *Proc. 59th Technical and Operating Conference*, Chicago, (2005).
9. Z. li, B.L. Ferguson, X. Sun and P. Bauerle, 'Experiment and Simulation of Heat Treatment Results of C-Ring Test Specimen', In: *Proc. 23rd ASM Heat Treating Society Conference*, Pittsburgh, (2005) 245-252.
10. M. Teodorescu, J. Demurger and J. Wendenbaum, Comprehension of Cooling Distortion Mechanisms by the mean of F.E. Simulation, In: *Proc. 15th IFHTFE*, Vienne, (2006).